BMC Oral Health

RESEARCH

Open Access

Abutment connection structural changes in dual-retained and screw-retained metal-ceramic implant-supported restorations: an in vitro study, part I

Sareh Habibzadeh[1], Safoura Ghodsi[2], Marzieh Alikhasi[2], Seyed Ali Mosaddad[3,4] and Hosein Mohebbi[5*]

Abstract

Background This study sought to compare the rotational freedom and structural changes of abutment connections in dual-retained and screw-retained metal-ceramic implant restorations at different fabrication stages and following thermomechanical loading.

Methods Twenty metal-ceramic restorations were equally divided into two groups. Group 1 (G1) consisted of dual-retained restorations on prefabricated titanium abutments, while Group 2 (G2) comprised screw-retained restorations on UCLA chromium-cobalt overcast abutments. Specimens underwent 500 cycles of thermocycling and 500,000 cycles of mechanical loading. Changes in connection dimensions and rotational freedom were compared within and between the groups before- and post-loading. Statistical analyses were conducted using a generalized linear model (GLM). The significance level was set at $\alpha = 0.05$.

Results Initially, no significant differences in connection dimensions were observed between the groups ($P > .05$). After loading, G2 exhibited significantly smaller hexagon side lengths and diagonal measurements, along with increased hexagonal angle deformation and concentricity ($P < .001$) compared to G1. Rotational freedom was significantly greater in G2 compared to G1 both before and after thermomechanical loading ($P < .001$). G2 experienced significant dimensional changes before and after loading ($P < .001$), whereas G1 showed no significant changes in connection dimensions pre- and post-loading ($P > .05$).

Conclusions Dual-retained restorations outperformed screw-retained ones with minimal connection alteration and higher rotational stability.

Keywords Dental implants, Dental prosthesis, Implant supported dental prosthesis, Prosthesis fitting, Single tooth dental implant

*Correspondence:
Hosein Mohebbi
hossein_mohebbi74@yahoo.com
[1]Dental Research Center, Dentistry Research Institute, Department of Prosthodontics, School of Dentistry, International Campus, Tehran University of Medical Sciences, Tehran, Iran
[2]Dental Research Center, Dentistry Research Institute, Department of Prosthodontics, Tehran University of Medical Sciences, Tehran, Iran
[3]Department of Research Analytics, Saveetha Institute of Medical and Technical Sciences, Saveetha Dental College and Hospitals, Saveetha University, Chennai, India
[4]Department of Conservative Dentistry and Bucofacial Prosthesis, Faculty of Odontology, Complutense University of Madrid, Madrid, Spain
[5]Department of Prosthodontics, Faculty of Dentistry, AJA University of Medical Sciences, Tehran, Iran

Introduction

In dentistry, implant treatment is recognized for its commendable success rates, making it a reliable, safe, and predictable approach for rehabilitating edentulism in diverse clinical scenarios [1]. Various prosthetic options are at the disposal of clinicians when considering fixed single- or multi-unit implant-supported restorations. These include cement-retained, screw-retained, and dual-retained restorations, each possessing distinct characteristics that justify its application in specific scenarios [2]. The selection between these prostheses is a subject of debate among researchers, and consensus has yet to be reached [3, 4].

The advantages of cement-retained restorations include the ease of achieving passivity, enhanced aesthetics resulting from the absence of a screw access hole, and simpler occlusion control [3, 5, 6]. However, the use of this restoration type is restricted by the minimum required height for the restorative space (5 mm) [7]. Moreover, the primary drawback lies in the challenge of removing excess cement, which can result in biological complications [8].

The screw-retained type offers the benefit of retrievability, facilitating removal when necessary [3, 5]. However, this type encounters certain issues, such as screw loosening or fracture, difficulty in achieving a passive fit, disrupted natural occlusal morphology [9, 10], and aesthetic challenges [5, 11]. Typically, screw-retained restorations are fabricated using prefabricated universal casting long abutments (UCLA) [12], which come in two variants: (1) castable all-plastic and (2) overcast abutments with a plastic sleeve and a pre-machined metallic connection composed of either gold or base metal cobalt-chromium alloys, with an increasing trend towards the adoption of base metal connections due to the elevated gold cost. This type of connection is susceptible to corrosion [13, 14], as well as shape and dimensional alterations, surface roughness during the casting process, and further firing cycles throughout the fabrication process, having the potential to adversely impact the mechanical properties [15, 16].

Another type of implant restoration is known as cement-screw- or dual-retained restoration [17–20]. In this type, the crown is definitively cemented onto the abutment either extraorally or intraorally, and any excess cement is thoroughly removed. Subsequently, the crown-abutment assembly is screwed to the implant through an access hole in the crown using an abutment screw [19]. Finally, the access hole is sealed with resin composite [17, 21]. The use of a screw access hole in cement-retained restorations was first introduced as the "combination implant crown" by McGlumphy in 1992 [22]. Rajan and Gunaseelan (2004) employed this technique to attach a single-unit metal-ceramic crown to a customized cast abutment [17]. Uludag et al. also studied the dual-retained restoration design for fabricating multi-unit restorations on custom cast abutments [18, 21]. Dual-retained restorations, despite their shorter history of use compared to the other two types, claim improvements in biological and mechanical properties over cement-retained restorations, with benefits such as easier retrievability, elimination of issues related to excess cement, providing more reliable retention, suitability for limited interocclusal spaces, and the ability to use gingival depth for better emergence profile shaping, and over screw-retained restorations, with advantages such as improved passivity, simplified fabrication processes, the possibility of using standard abutments, and increased resistance to fracture due to the supportive effect of the intermediary cement [17]. In contrast to screw-retained restorations fabricated with UCLA abutments, the abutments utilized in these restorations do not undergo the thermal cycle associated with casting and porcelain firing, potentially impacting their fit and overall quality [23]. Disadvantages such as the potential for reduced crown retention and porcelain weakening due to the access hole have been cited for these restorations, yet studies have reported conflicting results [24–27]. Over 12 years, a total of 274 dual-retained restorations were evaluated by Nissan et al. They concluded that this design improves the long-term survival rates of restorations and reduces maintenance costs without raising the risk of porcelain fracture or screw loosening [28].

Most studies on dual-retained restorations have examined the effect of screw access hole location on fracture strength, often with inconsistent findings [10, 24–27, 29–33]. Other mechanical factors critical to long-term success—especially in dual-retained designs—remain underexplored. Additionally, research has largely focused on all-ceramic systems, despite the applicability of dual retention to conventional metal-ceramic restorations using standard abutments [33]. While Finite Element Analysis (FEA) has been used to assess stress distribution in implant restorations [34–36], data on the structural stability and rotational behavior of dual-retained metal-ceramic designs remain scarce. This study aimed to compare structural changes and rotational freedom between dual- and screw-retained metal-ceramic restorations under thermomechanical loading. The null hypothesis stated that there would be no significant differences between the two groups.

Materials and methods

An in vitro study was conducted to compare the mean differences in structural properties and rotational freedom between dual-retained (intervention group) and screw-retained (comparison group) metal-ceramic implant restorations at the initial assessment and

following thermomechanical loading. The required sample size was estimated using G*Power software (version 3.1, Heinrich-Heine-Universität Düsseldorf, Germany) based on the repeated measures ANOVA model. Assuming an effect size of 0.8, a correlation coefficient of 0.8, a Type I error rate of 5%, and a power of 90%, the estimated sample size was 18 specimens. To account for a 10% failure rate of the samples, the final sample size was determined to be 20 specimens (10 per group). The study was approved by the Ethics Committee at Tehran University of Medical Sciences, with the identifier IR.TUMS.DENTISTRY.REC.1401.057.

A rectangular cuboid master block was fabricated from cobalt-chromium (Co-Cr) alloy (Vera band, Albadent, Cordelia, CA, USA; Elastic modulus [E] ≈ 210 GPa), measuring 25 × 38 × 16 mm. Within this block, a central rectangular cuboid space (8 × 8 × 15 mm) flanked by two cylindrical cavities was created to mount acrylic maxillary second premolar and second molar teeth using auto-polymerized acrylic resin (Acropars, Marlic Medical Industries, Iran; Elastic modulus [E] ≈ 2.5–3.0 GPa). Twenty smaller metal blocks, constructed from the same alloy and sized to match the dimensions of the middle hole, were created to attach to the main block using screws from underneath; these smaller blocks, referred to as implant blocks, were intended for mounting the implants (Fig. 1). The occlusal surfaces of the acrylic teeth were oriented parallel to the horizon, and the teeth were embedded inside the acrylic to a depth, ensuring their cementoenamel junction (CEJ) remained above the acrylic surface. Implants, each measuring Ø4 × 10 mm and featuring an 11° conical and internal hex connection (IS-II Active Implant, Neobiotech, Seoul, Republic of Korea), were mounted perpendicularly to the horizon in the implant blocks by a surveyor using auto-polymerized resin, ensuring the implant platform was elevated 1 mm above the acrylic surface.

Ten restorations were fabricated on the implants in each of the dual-retained (G1) and screw-retained (G2) groups ($n = 10$ per group). In G1, straight prefabricated abutments with a diameter of 6.5 mm and a height of 4.5 mm (GH = 3 mm) (IS Cemented Abutment, Hex

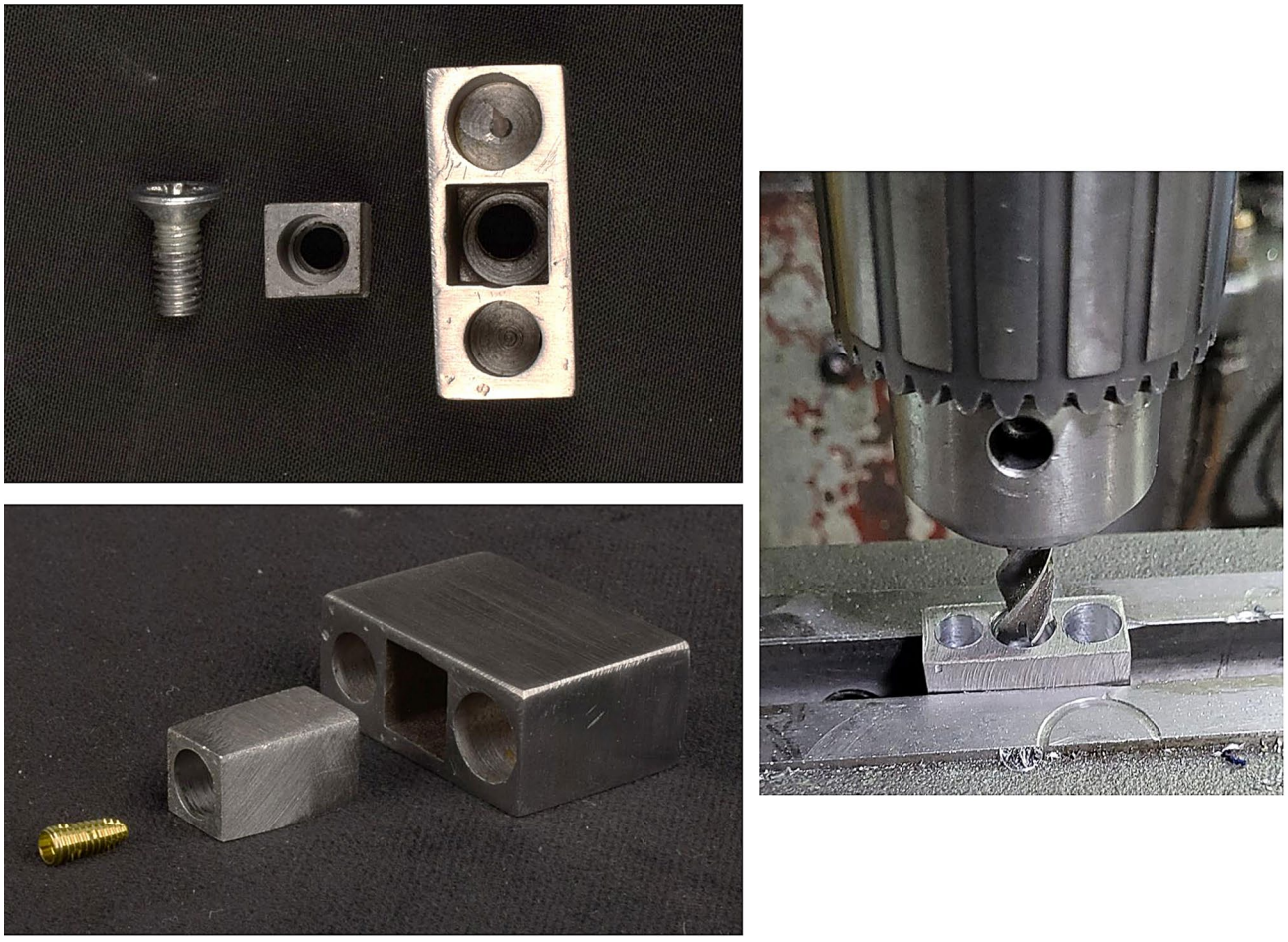

Fig. 1 A master model of a rectangular cuboid cobalt-chromium block, featuring a central rectangular cuboid cavity with two cylindrical spaces on either side

type, Neobiotech, Seoul, Republic of Korea) were utilized (Fig. 2A), upon which metal-ceramic dual-retained restorations were fabricated. In G2, UCLA overcast Co-Cr abutments (CCM UCLA Abutment, Neobiotech, Seoul, Republic of Korea) were employed to fabricate screw-retained metal-ceramic restorations (Fig. 2D). The restorations were modeled with the anatomy of the first maxillary molar using the same index.

Metallic frames were designed as follows: In G1, one of the corresponding abutments was scanned using a laboratory scanner (T510, MEDIT Corp, Seoul, Republic of Korea) and scan powder (Snow Scan Powder, Snow Rock Co., Japan). The frame, inclusive of the lingual collar, abutment screw access hole, and a cement space of 40 µm, was designed in CAD software (Exocad DentalCAD, Exocad, Darmstadt, Germany). In G2, a UCLA abutment was scanned similarly, and the frame designed for G1 was superimposed on the plastic cylinder. Both groups' frame patterns were then 3D printed (Fig. 2B and E) using resin material (JamgHe, Shenzhen Yongchanghe Technology Co., China). In the screw-retained group, the printed patterns were affixed to the plastic cylinders using wax, with both groups visually inspected for frame similarity (dimensions, lingual support, porcelain space). Finally, frames were fabricated using cobalt-chromium alloy in a casting furnace (Vera band, Albadent, Cordelia, CA, USA) (Fig. 2C and F). Following this, porcelain (Noritake, Kuraray, Tokyo, Japan) was applied on a frame from the dual-retained group with a thickness of 1 mm on axial surfaces and 1.5 mm on cusps and an access hole for the abutment screw. For the remaining samples in both groups, porcelain was applied using a silicone index and visual inspection on the mounted blocks. All laboratory procedures were carried out by a single technician who was blinded to the grouping and study design.

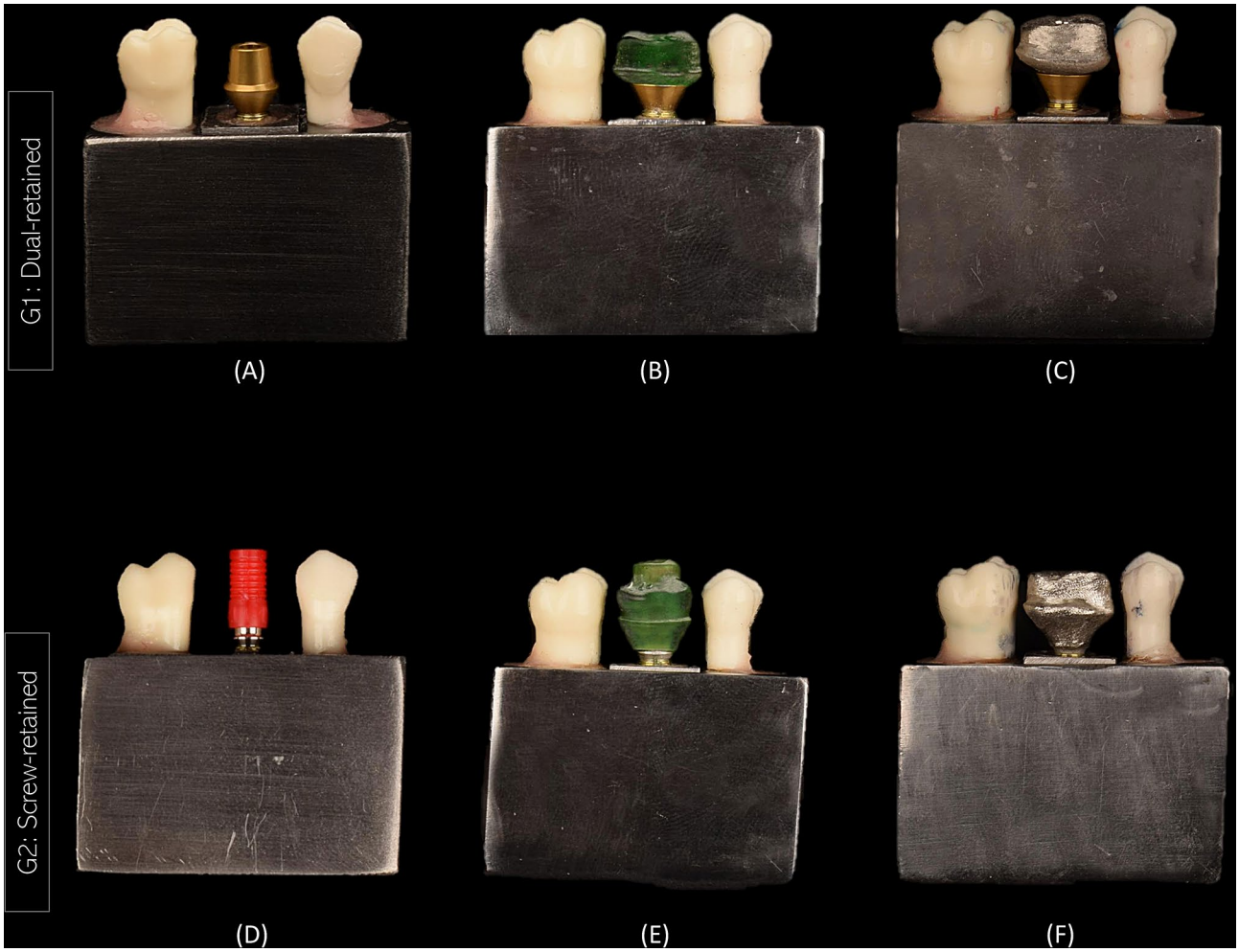

Fig. 2 (**A**) A straight prefabricated abutment used for the dual-retained restorations. (**B**) A 3D-printed resin pattern for casting the metallic frameworks of the dual-retained restorations. (**C**) The final cast frame for the dual-retained groups. (**D**) A UCLA abutment placed in the metal block for designing and fabricating screw-retained restorations. (**E**) A 3D-printed resin pattern for casting the metallic frames of the screw-retained restorations. (**F**) The cast metallic frames of the screw-retained restorations

The fabricated restorations were adjusted until complete seating was achieved. The crowns in G1 were cemented to the abutments using a dual-cure self-adhesive resin cement (TheraCem, BISCO, Illinois, USA) [29]. A micro brush was utilized to eliminate any excess cement. The crowns were then clamped for 10 min with force equivalent to finger pressure, after which any remaining excess cement was removed [30]. The abutment connection changes and rotational freedom were compared between the two groups of restorations before the commencement of fabrication stages (t_1) and after thermo-mechanical loading (t_2).

Subsequently, crown-abutment sets were torqued to 30 Ncm on the implants using a digital torque meter. This procedure was repeated after a 10-minute interval. One-third of the screw channel was filled with Teflon tape, and the remaining portion with a hybrid composite resin (Solafil, Trentdent, UK). Afterward, the samples underwent thermocycling (Vafae Industrial Factory, Qom, Iran), which involved 500 cycles alternating between 5 °C and 55 °C, with each temperature maintained for 30 s and a dwell (transition) time of 20 s. The resulting frequency was approximately 0.01 Hz [32], followed by mechanical loading (500 N force applied for 500,000 cycles, equivalent to two clinical years, focused on the center of the slightly flattened palatal cusp of the samples) [37] (Chewing simulator CS-4 SD Mechatronik, Feldkirchen, Germany). To ensure purely vertical loading without sliding effects on the oblique cusp surfaces, the spherical-shaped loading tip of the universal testing machine was precisely positioned perpendicular to the center of the flattened palatal cusp surface of each sample. Throughout the mechanical loading process, periodic visual inspections were conducted to confirm consistent force direction and absence of lateral displacement or sliding.

After opening the abutment screw on all specimens (t_2), the abutment connection and rotational freedom were re-evaluated in both groups. Four measurements were conducted at each stage for assessing changes in the abutment connection by using a Video Measuring Machine (VMS-2515 A, Shanghai Cany Precision Instrument Co., China) with a precision of 1 µm (Fig. 3A). These measurements included (1) the length of each side of the hexagon (L1-L6), (2) the connection diameter determined by the lengths of the short and long hypotenuses of the hexagon (T1-T2), (3) concentricity, which was calculated as the distance between the center of the hexagon and the center of the circle above it (O), and (4) deformation of the hexagonal angles, measured by the distance between the hypothetical intersection of adjacent sides to a point perpendicular to the actual intersection manifested as a curve (P1-P6) (Fig. 3B). To assess rotational freedom in each intended phase, the implants were secured with a clamp. A flat-head pin was affixed to either the abutments or restorations, which was then manually rotated clockwise and counterclockwise until resistance was encountered. A photograph was taken by a digital camera (D3300, Nikon, USA) positioned perpendicular to the set after each rotation. The total angles resulting from the rotation were measured using Digimizer Image Analysis Software, v. 6.3.0 (MedCalc Software Ltd, Ostend, Belgium). All measurements were conducted by a single experienced prosthodontist (S.G.), with over ten years of clinical and research experience. While intra- and inter-examiner reliability were not assessed due to the single-operator protocol, standardized digital tools and

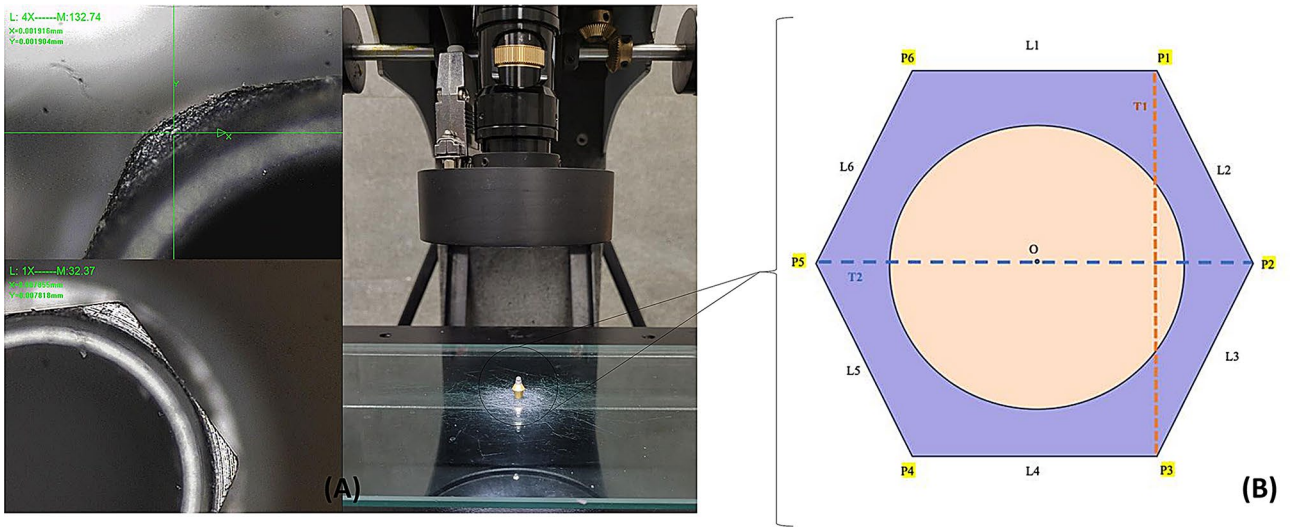

Fig. 3 (**A**) Evaluation of the abutment connection using a Video Measuring Machine. (**B**) Measurement variables related to changes in the abutment connection dimensions: L (Hexagonal side length), P (Hexagonal angle deformation), T1 (Short diagonal of the hexagon), T2 (Long diagonal of the hexagon), and O (Concentricity)

procedures were used to ensure consistency and reduce potential operator-related variability. The sequence of the study steps is schematically presented in Fig. 4.

Summary statistics for the study parameters were reported as mean ± standard deviation (SD). To compare the parameters both between and within groups, a generalized estimating equations (GEE) model was employed, followed by a least significant difference (LSD) post-hoc test. Statistical analyses were conducted using SPSS (IBM Corp. Released 2016. IBM SPSS Statistics for Windows, Version 24.0. Armonk, NY: IBM Corp.), with *P*-values less than 0.05 considered statistically significant.

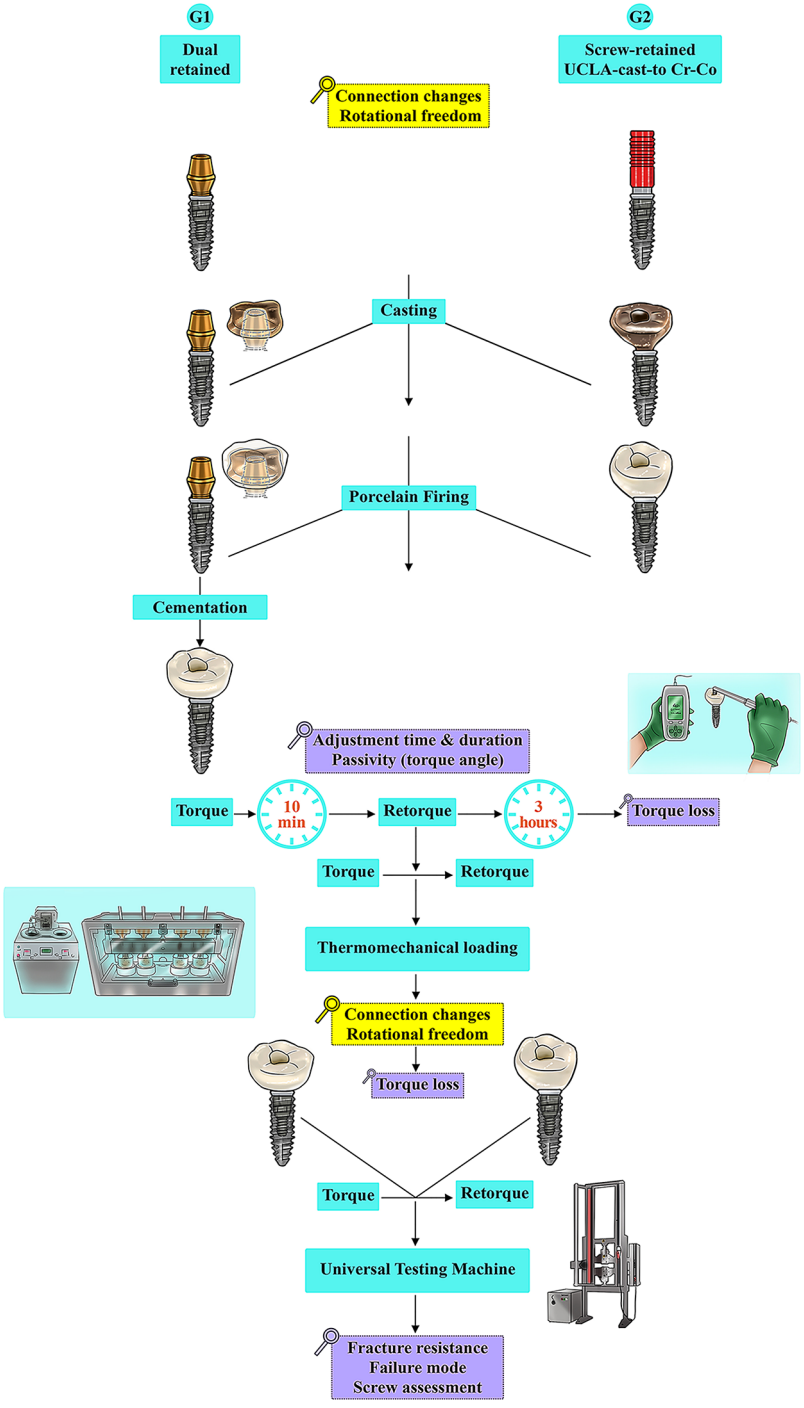

Fig. 4 Summary of the study methodology steps

Table 1 Descriptive information on study parameters

Study groups	Parameters	Before (Mean ± SD)	After (Mean ± SD)
Dual-retained	Average L	1.381 ± 0.016	1.381 ± 0.014
	Average P	0.015 ± 0.003	0.014 ± 0.003
	T1	2.498 ± 0.003	2.5 ± 0.004
	T2	2.885 ± 0.003	2.885 ± 0.003
	O	0.004 ± 0.001	0.005 ± 0.002
	RF	2.312 ± 0.088	2.316 ± 0.096
Screw-retained	Average L	1.385 ± 0.009	1.309 ± 0.045
	Average P	0.013 ± 0.002	0.027 ± 0.006
	T1	2.529 ± 0.094	2.485 ± 0.006
	T2	2.886 ± 0.003	2.865 ± 0.014
	O	0.005 ± 0.002	0.017 ± 0.008
	RF	2.531 ± 0.134	3.303 ± 0.233

L, Hexagonal side length; P, Hexagonal angle deformation; T1, Short diagonal of the hexagon; T2, Long diagonal of the hexagon; O, Concentricity; RF, Rotational freedom, SD, Standard Deviation

Table 2 Inter- and intra-group comparisons regarding each study parameter

Parameter	Comparison	MD	95% CI		*P*-value
			L	U	
L	Screw Before - Screw After	0.076	0.047	0.105	< 0.001
	Screw Before - Dual Before	0.004	-0.007	0.015	0.482
	Screw After - Dual After	-0.071	-0.099	-0.044	< 0.001
	Dual Before - Dual After	0.001	-0.004	0.005	0.701
P	Screw Before - Screw After	-0.014	-0.018	-0.010	< 0.001
	Screw Before - Dual Before	-0.001	-0.004	0.001	0.286
	Screw After - Dual After	0.013	0.009	0.017	< 0.001
	Dual Before - Dual After	0.001	-0.001	0.001	0.539
T1	Screw Before - Screw After	0.045	-0.010	0.099	0.108
	Screw Before - Dual Before	0.031	-0.024	0.087	0.268
	Screw After - Dual After	-0.015	-0.019	-0.011	< 0.001
	Dual Before - Dual After	-0.002	-0.003	0.001	0.054
T2	Screw Before - Screw After	0.021	0.012	0.029	< 0.001
	Screw Before - Dual Before	0.001	-0.002	0.003	0.609
	Screw After - Dual After	-0.020	-0.028	-0.012	< 0.001
	Dual Before - Dual After	0.001	-0.001	0.001	0.881
O	Screw Before - Screw After	-0.013	-0.017	-0.008	< 0.001
	Screw Before - Dual Before	0.001	-0.001	0.002	0.149
	Screw After - Dual After	0.012	0.007	0.017	< 0.001
	Dual Before - Dual After	-0.001	-0.003	0.001	0.104
RF	Screw Before - Screw After	-0.772	-0.936	-0.608	< 0.001
	Screw Before - Dual Before	0.219	0.125	0.313	< 0.001
	Screw After - Dual After	0.987	0.839	1.135	< 0.001
	Dual Before - Dual After	-0.004	-0.048	0.040	0.859

L, Hexagonal side length; P, Hexagonal angle deformation; T1, Short diagonal of the hexagon; T2, Long diagonal of the hexagon; O, Concentricity; RF, Rotational freedom; MD, Mean Difference; CI, Confidence Interval; L, Lower Bound; U, Upper Bound

Results

Table 1 presents the descriptive statistics of the study parameters, categorized by the intervention group before and after the thermomechanical loading. The results of the GEE model are presented in Table 2. The model findings indicated that the average L significantly decreased in G2 ($P<.001$), while no significant changes were observed in G1 ($P=.701$). Additionally, between-group comparisons showed no significant differences at t_1 ($P=.482$). However, after loading (t_2), the average L was significantly lower in G2 compared to G1 ($P<.001$) (Fig. 5A).

The model also revealed a significant increase in the average P for G2 ($P<.001$), whereas G1 showed no statistically significant changes ($P=.539$). Between-group comparisons indicated no significant difference at t_1 regarding the average P ($P=.286$). Nonetheless, at t_2, the average P was significantly higher in G2 ($P<.001$) (Fig. 5B).

For T1, a significant difference was observed between the groups after thermomechanical loading ($P<.001$), with the average T1 being lower in G2 (Fig. 5C). The model results also showed a significant decrease in the average T2 in G2 ($P<.001$), while G1 exhibited no significant changes ($P=.881$). Moreover, between-group comparisons showed no significant differences before thermomechanical loading ($P=.609$). However, after loading, the average T2 was significantly lower in G2 compared to G1 ($P<.001$) (Fig. 5D).

The model indicated a significant increase in the average O in G2 ($P<.001$), while no statistically significant changes were observed in G1 ($P=.104$). Between-group comparisons revealed no significant difference at t_1 ($P=.149$). However, after cycling (t_2), the average O was significantly higher in G2 ($P<.001$) (Fig. 5E).

Finally, the model demonstrated a significant increase in the average RF in G2 ($P<.001$), whereas G1 exhibited no significant changes ($P=.859$). Between-group comparisons showed significantly higher RF in G2 than in G1 both before and after thermomechanical loading ($P<.001$) (Fig. 5F).

Discussion

One of the most critical factors contributing to complications in implant-based restorations is the incompatibility between the abutment connection area and the implant [38]. When this connection is compromised, stress concentration in the abutment-implant interface increases, potentially leading to mechanical or biological complications that can impact the long-term success of the restoration or implant [39]. This study aimed to advance the understanding of the structural integrity of abutment connections in metal-ceramic implant restorations, focusing on dual- and screw-retained designs. The results indicated no significant differences between the groups before thermomechanical loading, except for rotational freedom. However, the null hypothesis was partially rejected after loading, as substantial differences emerged between the groups.

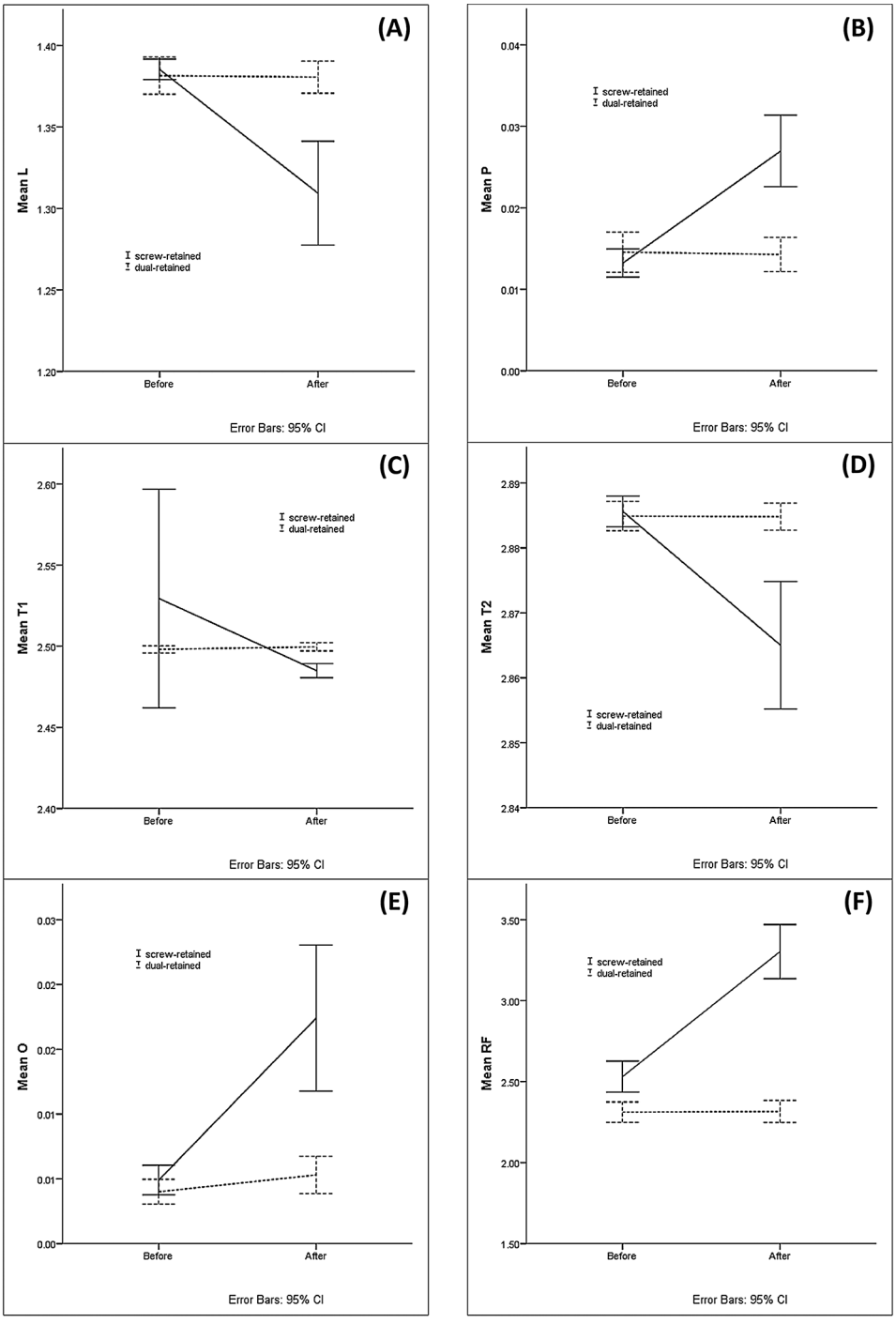

Fig. 5 Changes before and after thermomechanical loading in (**A**) Mean "L," (**B**) Mean "P," (**C**) "T1," (**D**) "T2," (**E**) "O," (**F**) "RF," based on the intervention group. L, Hexagonal side length; P, Hexagonal angle deformation; T1, Short diagonal of the hexagon; T2, Long diagonal of the hexagon; O, Concentricity; RF, Rotational freedom

In the initial phase of the study, no significant differences were observed between restorations concerning key connection parameters, which can be attributed to the precision of the manufacturing processes employed for both groups [40], indicating that both restoration types were initially comparable in their structural integrity and fit. However, the one notable exception was rotational freedom, which was significantly greater in the screw-retained group even before the onset of fabrication steps. This difference in rotational freedom can be attributed to the intrinsic design and material characteristics of the abutments used [41]. G1 utilized prefabricated

titanium abutments, which are known for their precision machining and tight tolerances [42–44]. Titanium, being a highly biocompatible and ductile material, allows for the manufacturing of abutment connections with minimal rotational freedom [45, 46]. The machining process for titanium abutments is optimized to achieve extremely accurate dimensions, ensuring a snug fit that minimizes any rotational movement [47]. G2 employed UCLA abutments made from Co-Cr alloy. Although these abutments were also precisely machined, the physical properties of Co-Cr differ from those of titanium. Co-Cr is a harder and less ductile material [48], which, despite the precision machining, can result in slightly greater manufacturing tolerances [49]. These minor differences in fit can lead to an increase in rotational freedom, as the connection between the abutment and the implant may not be as precise as that achieved with titanium.

After thermomechanical loading, significant differences emerged between the groups, with G2 exhibiting considerable changes in connection dimensions, such as reduced hexagon side lengths and diagonals, increased hexagonal angle deformation, and concentricity. These alterations in G2 can be attributed to the cumulative effects of the multiple fabrication steps involved in fabricating screw-retained restorations [50, 51]. Each step, including casting, porcelain firing, subsequent glazing, finishing, and polishing, introduces the potential for dimensional changes due to thermal expansion, shrinkage, and potential distortions [39]. These factors, coupled with the stresses imposed by thermomechanical loading [52], likely contributed to the observed dimensional changes in G2. In contrast, the dual-retained restorations in G1, which utilized prefabricated abutments without the need for the additional casting and firing steps involved in G2, exhibited minimal changes in connection dimensions, emphasizing the stability and precision of this design under loading stresses [53]. Similar to the results, In Malaguti et al.'s study [54], the initial mean distances between opposite sides were identical for both the hexagonal connections of the cemented abutment and the UCLA abutment with the prefabricated connection. However, after casting, the dimensions of the UCLA abutment connection were found to be smaller.

The findings of the present study are consistent with previous finite element analyses (FEA), highlighting the significance of stress distribution within implant-supported restorations. FEA studies have emphasized that material choice, implant-abutment connection type, and restorative design significantly influence the internal stresses generated under occlusal loading, potentially affecting the structural stability of restorations [34–36]. The observed superior dimensional stability and reduced rotational freedom in dual-retained restorations in this study may reflect more favorable internal stress distribution patterns, which corroborate the insights gained from these computational analyses.

The intra-group comparisons further reinforce the differential impact of the restoration design on connection stability. In the screw-retained group, significant changes were observed in all measured parameters after thermomechanical loading, indicating that the stresses induced by the fabrication steps, including oxidation and heat treatment, and loading process, exacerbated its dimensional integrity [52, 55–58]. Similarly, de Vasconcelos et al. [52] demonstrated that thermomechanical cyclic loading negatively influenced the misfit of cast abutments. On the other hand, the dual-retained group showed no significant changes before and after loading, possibly due to several key factors. First, the use of prefabricated titanium abutments, manufactured with high precision, ensured tight tolerances and minimized variability, resulting in a stable fit between the abutment and the implant [59]. Titanium's excellent mechanical and thermal properties, including a low coefficient of thermal expansion [60], contributed to maintaining the integrity of the connection dimensions during the thermomechanical loading process. Second, unlike G2, G1's absence of multiple fabrication steps further preserved dimensional stability. The precise fit of the prefabricated abutments minimized the potential for microgaps or misalignments, ensuring the implant-abutment interface remained unchanged even under mechanical stresses [59]. Collectively, these factors—precision in manufacturing, material resilience, absence of complex fabrication steps, and the stability of the dual-retained design—contributed to the superior performance and dimensional stability of G1 restorations under thermomechanical loading.

Clinically, the study's results have significant implications. Key connection measurements such as hexagonal side lengths, hexagonal angle deformation, and hexagon diagonals are critical in ensuring the mechanical stability of implant-supported restorations [61]. The reduced hexagonal side lengths and increased angle deformation in G2 indicate a loss of structural integrity, which could potentially compromise the stability of the restoration over time [62, 63]. Concentricity is another crucial parameter, as deviations can lead to uneven stress distribution at the implant-abutment interface, increasing the risk of mechanical complications such as screw loosening or fracture [64]. The observed increase in rotational freedom in G2, both before and after loading, is particularly concerning as it suggests that screw-retained restorations may be more prone to micromovements, leading to increased wear and potential failure of the abutment connection over time [65]. This result contrasts with the findings of Vigolo et al., who demonstrated that both gold-machined UCLA-type abutments and CAD/CAM titanium abutments consistently exhibited a similar

degree of rotational freedom between the implant and abutment. However, this discrepancy may be attributed to the use of a precious metal abutment connection in the gold UCLA abutments, which differs in material characteristics from the Co-Cr UCLA abutments [66]. In a similar study, Kano et al. demonstrated that the casting stage significantly increased the rotational freedom of the UCLA abutment with a prefabricated connection compared to the prefabricated abutment [16]. In contrast to the study by Kano et al. [16], which investigated simplified abutments on external hex implants without prosthetic restoration or loading, the present study utilized internal hex conical implants, clinically representative metal-ceramic restorations, and comprehensive fabrication and loading protocols. These methodological differences enhance the relevance of the findings to clinical scenarios. The degree of abutment rotational freedom in an implant is a significant factor in the long-term stability of the connection between these two components [61]. Deformation in the anti-rotation area of the implant abutment can lead to mechanical complications in the implant [65]. Surface irregularities and changes in the form of the connection increase rotational freedom, which in turn reduces the fit of the abutment implant and leads to loosening or fracturing of the abutment screw [63, 67]. The presence or creation of a micro gap directly causes microleakage and bacterial colonization [68], resulting in mechanical degradation of the implant and increased micromotion of the restoration, thus creating a defective cycle in which bone destruction by bacterial toxins or due to mechanical degradation of the implant is accelerated in the osseointegrated area [69, 70]. The maximum clinically acceptable rotational freedom is reported to be 5 degrees. In the present study, after thermomechanical loading, the rotational freedom of the abutments in both the dual-retained and screw-retained groups remained within this acceptable range [71]. From a clinical perspective, the findings of this study suggest that dual-retained restorations may be advantageous in situations where enhanced stability is required, such as in high occlusal load zones (e.g., molar regions) or when vertical restorative space is limited. Their combined retention approach enables the use of prefabricated abutments with simplified cementation and retrievability, potentially offering a more stable and practical solution compared to screw-retained designs, which may be vulnerable to structural deformation under functional loading. It should be emphasized that the clinical significance suggested by the results of this study is theoretical and based solely on the observed in vitro outcomes. Therefore, caution must be exercised when translating these findings directly into clinical practice, and further clinical trials are required to validate these conclusions.

Despite the additional findings provided by this study, several limitations must be acknowledged. Firstly, the study was conducted in vitro, and while the thermomechanical loading aimed to simulate clinical conditions, it cannot fully replicate the complex oral environment, including factors such as saliva, temperature fluctuations, and varying occlusal forces. Future studies with larger sample sizes and in vivo evaluations are necessary to confirm the clinical relevance of these findings. Moreover, the study focused on metal-ceramic restorations, and the results may not be directly applicable to all-ceramic restorations, which have different material properties and behavior under loading. Although the implant-abutment connection geometry remains constant, the type of restorative material and associated fabrication technique may influence the structural integrity of the connection. In metal-ceramic restorations, the casting of the metal framework introduces high temperatures, centrifugal forces, and potential distortions that can affect the fit of the connection. In contrast, all-ceramic restorations often employ pressing or CAD/CAM techniques, which involve distinct thermal profiles, processing durations, and manufacturing approaches, potentially resulting in varying mechanical behaviors and stress distributions. Lastly, the long-term effects of cyclic loading beyond the 500,000 cycles applied in this study remain to be explored, as real-world restorations are subjected to millions of cycles over their lifespan.

Conclusions

Within the limitations of this in vitro study, the following conclusions were drawn:

1. Dual-retained metal-ceramic implant restorations exhibited superior dimensional stability compared to screw-retained restorations following thermomechanical loading.
2. Dual-retained restorations demonstrated significantly lower rotational freedom relative to screw-retained restorations after loading.
3. Screw-retained restorations experienced significant dimensional changes and increased rotational freedom following thermomechanical loading, indicating potential vulnerability under mechanical stress conditions.

Acknowledgements
None.

Author contributions
Conceptualization: S.G., S.H., and H.M.; Methodology: S.G., M.A., and H.M.; Software: H.M. and S.A.M.; Validation: S.G., S.H., and M.A.; Formal analysis: H.M. and S.G.; Investigation: H.M. and S.H.; Resources: H.M. and S.G.; Data Curation: H.M. and S.G.; Writing - Original Draft: S.A.M and H.M.; Writing - Review & Editing: S.A.M. and S.G.; Visualization: H.M. and S.A.M.; Supervision: S.G. and S.H.; Project administration: S.G. All authors have read and approved the published version of the manuscript.

Funding
This study received no external funding.

Data availability
The data presented in this study are available on request from the corresponding author.

Declarations

Ethics approval and consent to participate
The study was approved by the Ethics Committee at Tehran University of Medical Sciences, with the identifier IR.TUMS.DENTISTRY.REC.1401.057.

Consent for publication
Not applicable.

Competing interests
The authors declare no competing interests.

Received: 21 February 2025 / Accepted: 24 April 2025
Published online: 30 April 2025

References

1. Sartoretto SC, Shibli JA, Javid K, Cotrim K, Canabarro A, Louro RS et al. Comparing the Long-Term success rates of tooth preservation and dental implants: A critical review. J Funct Biomater. 2023;14(3).
2. Michalakis KX, Hirayama H, Garefis PD. Cement-retained versus screw-retained implant restorations: a critical review. Int J Oral Maxillofac Implants. 2003;18(5):719–28.
3. Shadid R, Sadaqa N. A comparison between screw- and cement-retained implant prostheses. A literature review. J Oral Implantol. 2012;38(3):298–307.
4. Gómez-Polo M, Ortega R, Gómez-Polo C, Celemin A, Del Rio Highsmith J. Factors affecting the decision to use cemented or Screw-Retained fixed Implant-Supported prostheses: A critical review. Int J Prosthodont. 2018;31(1):43–54.
5. Wittneben JG, Joda T, Weber HP, Brägger U. Screw retained vs. cement retained implant-supported fixed dental prosthesis. Periodontol 2000. 2017;73(1):141–51.
6. Chee W, Jivraj S. Screw versus cemented implant supported restorations. Br Dent J. 2006;201(8):501–7.
7. Makke A, Homsi A, Guzaiz M, Almalki A. Survey of screw-retained versus cement-retained implant restorations in Saudi Arabia. Int J Med Dent. 2017;27(3):1–5.
8. Korsch M, Robra BP, Walther W. Predictors of excess cement and tissue response to fixed implant-supported dentures after cementation. Clin Implant Dent Relat Res. 2015;17(1):45–53.
9. Torrado E, Ercoli C, Al Mardini M, Graser GN, Tallents RH, Cordaro L. A comparison of the porcelain fracture resistance of screw-retained and cement-retained implant-supported metal-ceramic crowns. J Prosthet Dent. 2004;91(6):532–7.
10. Zarone F, Sorrentino R, Traini T, Caputi S. Fracture resistance of implant-supported screw-versus cement-retained porcelain fused to metal single crowns: SEM fractographic analysis. Dent Mater. 2007;23(3):296–301.
11. AlHelal A, Kattadiyil MT, Clark JL, AlBader B. Diagnostic classification and design considerations for Implant-Supported fixed partial dentures and screw access channel: the ABC/PBC and SAC classifications. Int J Prosthodont. 2017;30(5):490–5.
12. Lewis S, Beumer J 3rd, Hornburg W, Moy P. The UCLA abutment. Int J Oral Maxillofac Implants. 1988;3(3):183–9.
13. Pulskamp FE. A comparison of the casting accuracy of base metal and gold alloys. J Prosthet Dent. 1979;41(3):272–6.
14. Son M-K, Choe H-C, Chung C-H. Corrosion behavior between dental implant abutment and cast gold alloy. Met Mater Int. 2004;10(2):153–9.
15. Kano SC, Binon P, Bonfante G, Curtis DA. Effect of casting procedures on screw loosening in UCLA-type abutments. J Prosthodont. 2006;15(2):77–81.
16. Kano SC, Binon PP, Bonfante G, Curtis DA. The effect of casting procedures on rotational misfit in castable abutments. Int J Oral Maxillofac Implants. 2007;22(4):575–9.
17. Rajan M, Gunaseelan R. Fabrication of a cement-and screw-retained implant prosthesis. J Prosthet Dent. 2004;92(6):578–80.
18. Uludag B, Celik G. Fabrication of a cement- and screw-retained multiunit implant restoration. J Oral Implantol. 2006;32(5):248–50.
19. Proussaefs P, AlHelal A. The combination prosthesis: A digitally designed retrievable cement-and screw-retained implant-supported prosthesis. J Prosthet Dent. 2018;119(4):535–9.
20. AlHelal A, Kattadiyil MT, AlBader B, Clark JL. A protocol for Screw-Retrievable, Cement-Retained, Implant-Supported fixed partial dentures. Int J Prosthodont. 2017;30(6):577–80.
21. Uludag B, Ozturk O, Celik G, Goktug G. Fabrication of a retrievable cement- and screw-retained implant-supported zirconium fixed partial denture: a case report. J Oral Implantol. 2008;34(1):59–62.
22. McGlumphy E, Papazoglou E, Riley R. The combination implant crown: a cement-and screw-retained restoration. Compendium. 1992;13(1):34–6.
23. Chee WW, Torbati A, Albouy JP. Retrievable cemented implant restorations. J Prosthodont. 1998;7(2):120–5.
24. Derafshi R, Farzin M, Taghva M, Heidary H, Atashkar B. The effects of new design of access hole on porcelain fracture resistance of Implant-Supported crowns. J Dent (Shiraz). 2015;16(1 Suppl):61–7.
25. Mokhtarpour H, Eftekhar Ashtiani R, Mahshid M, Tabatabaian F, Alikhasi M. Effect of screw access hole Preparation on fracture load of implant-supported zirconia-based crowns: an in vitro study. J Dent Res Dent Clin Dent Prospects. 2016;10(3):181–8.
26. Hussien ANM, Rayyan MM, Sayed NM, Segaan LG, Goodacre CJ, Kattadiyil MT. Effect of screw-access channels on the fracture resistance of 3 types of ceramic implant-supported crowns. J Prosthet Dent. 2016;116(2):214–20.
27. Honda J, Komine F, Kamio S, Taguchi K, Blatz MB, Matsumura H. Fracture resistance of implant-supported screw-retained zirconia-based molar restorations. Clin Oral Implants Res. 2017;28(9):1119–26.
28. Nissan J, Snir D, Rosner O, Kolerman R, Chaushu L, Chaushu G. Reliability of retrievable cemented implant-supported prostheses. J Prosthet Dent. 2016;115(5):587–91.
29. Malpartida-Carrillo V, Tinedo-López PL, Ortiz-Culca F, Guerrero ME, Amaya-Pajares SP, Özcan M. Fracture resistance of Cement-retained, Screw-retained, and combined Cement-and Screw-retained Metal-ceramic Implant-supported molar restorations. J Contemp Dent Pract. 2020;21(8):868–73.
30. Nogueira LBLV, Moura CDVS, Francischone CE, Valente VS, Alencar SMM, Moura WL, Soares Martins GA. Fracture strength of implant-supported ceramic crowns with customized zirconia abutments: screw retained vs. cement retained. J Prosthodont. 2016;25(1):49–53.
31. Shadid RM, Abu-Naba'a L, Al-Omari WM, Asfar KR, El Masoud BM. Effect of an occlusal screw-access hole on the fracture resistance of permanently cemented implant crowns: a laboratory study. Int J Prosthodont. 2011;24(3):267–9.
32. Al-Omari WM, Shadid R, Abu-Naba'a L, Masoud BE. Porcelain fracture resistance of screw-retained, cement-retained, and screw-cement-retained implant-supported metal ceramic posterior crowns. J Prosthodont. 2010;19(4):263–73.
33. Karl M, Graef F, Taylor TD, Heckmann SM. In vitro effect of load cycling on metal-ceramic cement- and screw-retained implant restorations. J Prosthet Dent. 2007;97(3):137–40.
34. Ausiello P, Ciaramella S, De Benedictis A, Lanzotti A, Tribst JPM, Watts DC. The use of different adhesive filling material and mass combinations to restore class II cavities under loading and shrinkage effects: a 3D-FEA. Comput Methods Biomech Biomed Engin. 2021;24(5):485–95.
35. Lemos CAA, Verri FR, Noritomi PY, de Souza Batista VE, Cruz RS, de Luna Gomes JM, et al. Biomechanical evaluation of different Implant-Abutment connections, retention systems, and restorative materials in the Implant-Supported single crowns using 3D finite element analysis. J Oral Implantol. 2022;48(3):194–201.
36. Aboelfadl A, Keilig L, Ebeid K, Ahmed MAM, Nouh I, Refaie A, Bourauel C. Biomechanical behavior of implant retained prostheses in the posterior maxilla using different materials: a finite element study. BMC Oral Health. 2024;24(1):455.
37. Ozdiler A, Dayan SC, Gencel B, Ozkol GI. Reverse torque values of abutment screws after dynamic loading: effects of sealant agents and the taper of conical connections. J Oral Implantology. 2021;47(4):287–93.
38. Block MS. Evidence-Based criteria for an ideal abutment implant Connection—A narrative review. J Oral Maxillofac Surg. 2022;80(10):1670–5.
39. Ramalho IS, Bergamo ETP, Witek L, Coelho PG, Lopes ACO, Bonfante EA. Implant-abutment fit influences the mechanical performance of single-crown prostheses. J Mech Behav Biomed Mater. 2020;102:103506.

40. Byrne D, Houston F, Cleary R, Claffey N. The fit of cast and premachined implant abutments. J Prosthet Dent. 1998;80(2):184–92.
41. Bédouin Y, Lefrançois E, Salomon JP, Auroy P. Abutment rotational freedom on five implant systems with different internal connections. J Prosthet Dent. 2023;129(3):433–9.
42. Ortorp A, Jemt T, Bäck T, Jälevik T. Comparisons of precision of fit between cast and CNC-milled titanium implant frameworks for the edentulous mandible. Int J Prosthodont. 2003;16(2):194–200.
43. Wu H, Chen X, Kong L, Liu P. Mechanical and biological properties of titanium and its alloys for oral implant with Preparation techniques: A review. Materials. 2023;16(21):6860.
44. Ohkubo C, Watanabe I, Ford JP, Nakajima H, Hosoi T, Okabe T. The machinability of cast titanium and Ti–6Al–4V. Biomaterials. 2000;21(4):421–8.
45. Lops D, Meneghello R, Sbricoli L, Savio G, Bressan E, Stellini E. Precision of the connection between implant and standard or Computer-Aided Design/Computer-Aided manufacturing abutments: A novel evaluation method. Int J Oral Maxillofac Implants. 2018;33(1):23–30.
46. Silva RCS, Agrelli A, Andrade AN, Mendes-Marques CL, Arruda IRS, Santos LRL et al. Titanium dental implants: an overview of applied nanobiotechnology to improve biocompatibility and prevent infections. Mater (Basel). 2022;15(9).
47. Lee JH, Park JM, Park EJ, Koak JY, Kim SK, Heo SJ. Comparison of customized abutments made from titanium and a machinable precious alloy. Int J Oral Maxillofac Implants. 2016;31(1):92–100.
48. Moharrami N, Langton DJ, Sayginer O, Bull SJ. Why does titanium alloy wear Cobalt Chrome alloy despite lower bulk hardness: A nanoindentation study? Thin Solid Films. 2013;549:79–86.
49. Zaman HA, Sharif S, Kim D-W, Idris MH, Suhaimi MA, Tumurkhuyag Z. Machinability of Cobalt-based and Cobalt chromium molybdenum Alloys - A review. Procedia Manuf. 2017;11:563–70.
50. Queiroz DA, Hagee N, Lee DJ, Zheng F. The behavior of a zirconia or metal abutment on the implant-abutment interface during Cyclic loading. J Prosthet Dent. 2020;124(2):211–6.
51. Camargos Gde V, do Prado CJ, das Neves FD, Sartori IA. Clinical outcomes of single dental implants with external connections: results after 2 to 13 years. Int J Oral Maxillofac Implants. 2012;27(4):935–44.
52. de Vasconcelos JEL, de Matos JDM, Queiroz DA, Lopes G, de Lacerda B, Bottino MA et al. Implant-Abutment misfit after Cyclic loading: an in vitro experimental study. Mater (Basel). 2022;15(15).
53. Al-Thobity AM. Titanium base abutments in implant prosthodontics: A literature review. Eur J Dent. 2022;16(1):49–55.
54. Malaguti G, Denti L, Bassoli E, Franchi I, Bortolini S, Gatto A. Dimensional tolerances and assembly accuracy of dental implants and machined versus cast-on abutments. Clin Implant Dent Relat Res. 2011;13(2):134–40.
55. Haralur SB, Hamdi OA, Al-Shahrani AA, Alhasaniah S. The effect of casting ring liner length and prewetting on the marginal adaptation and dimensional accuracy of full crown castings. J Int Soc Prev Community Dentistry. 2017;7(1):52–7.
56. Zeng L, Zhang Y, Liu Z, Wei B. Effects of repeated firing on the marginal accuracy of Co-Cr copings fabricated by selective laser melting. J Prosthet Dent. 2015;113(2):135–9.
57. Giti R, Hosseinpour Aghaei M, Mohammadi F. The effect of repeated porcelain firings on the marginal fit of millable and conventional casting alloys. PLoS ONE. 2023;18(10):e0275374.
58. Pereira PHS, Amaral M, Baroudi K, Vitti RP, Nassani MZ, Silva-Concílio LRD. Effect of implant platform connection and abutment material on removal torque and implant hexagon plastic deformation. Eur J Dent. 2019;13(3):349–53.
59. Alonso-Pérez R, Bartolomé JF, Fraile C, Pradíes G. Original versus nonoriginal cast-to-gold abutment-implant connection: analysis of the internal fit and long-term fatigue performance. J Prosthet Dent. 2021;126(1):94.e1–e9.
60. Marin E, Lanzutti A. Biomedical applications of titanium alloys: A comprehensive review. Materials. 2024;17(1):114.
61. Vinhas AS, Aroso C, Salazar F, López-Jarana P, Ríos-Santos JV, Herrero-Climent M. Review of the mechanical behavior of different Implant-Abutment connections. Int J Environ Res Public Health. 2020;17(22).
62. Berberi A, Maroun D, Kanj W, Amine EZ, Philippe A. Micromovement evaluation of original and compatible abutments at the Implant-abutment interface. J Contemp Dent Pract. 2016;17(11):907–13.
63. Vigolo P, Majzoub Z, Cordioli G. Measurement of the dimensions and abutment rotational freedom of gold-machined 3i UCLA-type abutments in the as-received condition, after casting with a noble metal alloy and porcelain firing. J Prosthet Dent. 2000;84(5):548–53.
64. Choi S, Kang YS, Yeo I-SL. Influence of Implant–Abutment connection biomechanics on biological response: A literature review on interfaces between implants and abutments of titanium and zirconia. Prosthesis. 2023;5(2):527–38.
65. Kwon JH, Han CH, Kim SJ, Chang JS. The change of rotational freedom following different insertion torques in three implant systems with implant driver. J Adv Prosthodont. 2009;1(1):37–40.
66. Vigolo P, Fonzi F, Majzoub Z, Cordioli G. Evaluation of gold-machined UCLA-type abutments and CAD/CAM titanium abutments with hexagonal external connection and with internal connection. Int J Oral Maxillofac Implants. 2008;23(2):247–52.
67. Vigolo P, Givani A, Majzoub Z, Cordioli G. Cemented versus screw-retained implant-supported single-tooth crowns: a 4-year prospective clinical study. Int J Oral Maxillofac Implants. 2004;19(2):260–5.
68. Ramos MB, Pegoraro LF, Takamori E, Coelho PG, Silva TL, Bonfante EA. Evaluation of UCLA implant-abutment sealing. Int J Oral Maxillofac Implants. 2014;29(1):113–20.
69. Sahin C, Ayyildiz S. Correlation between microleakage and screw loosening at implant-abutment connection. J Adv Prosthodont. 2014;6(1):35–8.
70. Liu Y, Wang J. Influences of microgap and micromotion of implant-abutment interface on marginal bone loss around implant neck. Arch Oral Biol. 2017;83(5):153–60.
71. Junqueira MC, Silva TE, Ribeiro RF, Faria AC, Macedo AP, de Almeida RP. Abutment rotational freedom evaluation of external hexagon single-implant restorations after mechanical cycling. Clin Implant Dent Relat Res. 2013;15(6):927–33.

Publisher's note